remote sensing

MDPI

Review

A Review of Selected Applications of GNSS CORS and Related Experiences at the University of Palermo (Italy)

Claudia Pipitone [1], Antonino Maltese [2], Mauro Lo Brutto [2] and Gino Dardanelli [2,*]

[1] Istituto Nazionale di Geofisica e Vulcanologia, Osservatorio Vesuviano, 80124 Napoli, Italy; claudia.pipitone@ingv.it
[2] Department of Engineering, Università degli Studi di Palermo, 90128 Palermo, Italy; antonino.maltese@unipa.it (A.M.); mauro.lobrutto@unipa.it (M.L.B.)
* Correspondence: gino.dardanelli@unipa.it

Abstract: Services from the Continuously Operating Reference Stations (CORS) of the Global Navigation Satellite System (GNSS) provide data and insights to a range of research areas such as physical sciences, engineering, earth and planetary sciences, computer science, and environmental science. Even though these fields are varied, they are all linked through the GNSS operational application. GNSS CORS have historically been deployed for three-dimensional positioning but also for the establishment of local and global reference systems and the measurement of ionospheric and tropospheric errors. In addition to these studies, CORS is uncovering new, emerging scientific applications. These include real-time monitoring of land subsidence via network real-time kinematics (NRTK) or precise point positioning (PPP), structural health monitoring (SHM), earthquake and volcanology monitoring, GNSS reflectometry (GNSS-R) for mapping soil moisture content, precision farming with affordable receivers, and zenith total delay to aid hydrology and meteorology. The flexibility of CORS infrastructure and services has paved the way for new research areas. The aim of this study is to present a curated selection of scientific papers on prevalent topics such as network monitoring, reference frames, and structure monitoring (like dams), along with an evaluation of CORS performance. Concurrently, it reports on the scientific endeavours undertaken by the Geomatics Research Group at the University of Palermo in the realm of GNSS CORS over the past 15 years.

Keywords: GNSS; CORS; network; structures monitoring; accuracy

Citation: Pipitone, C.; Maltese, A.; Lo Brutto, M.; Dardanelli, G. A Review of Selected Applications of GNSS CORS and Related Experiences at the University of Palermo (Italy). *Remote Sens.* **2023**, *15*, 5343. https://doi.org/10.3390/rs15225343

Academic Editors: Giuseppe Casula and Michael E. Gorbunov

Received: 22 September 2023
Revised: 30 October 2023
Accepted: 7 November 2023
Published: 13 November 2023

1. Introduction

Since the 1970s, the evolution of electronic and computer technology, with the increasing miniaturisation of components, has influenced the construction of surveying instruments and techniques, and, on the other hand, scientific software developments have provided new surveying methodologies taking advantage of automatic calculation tools. As a consequence, geomatics surveying methodologies have undergone an unexpected development. In a few decades, for topographic surveying, we have witnessed a transition from optical-mechanical instruments, such as theodolites and tilting levels (associated with meta-grad rods) [1], to integrated electronic theodolites and Total Stations, able to measure both angles and distances, as well as perform calculations, with the possibility of remote monitoring. In the 1990s, the development of a *Global Positioning System* (GPS), an innovative integrated US system that uses, for the first time in modern history, a constellation of artificial satellites for topographic and geodetic surveying, was a true innovation in the field of geomatics. This system, originally made for military purposes of assisting navigation, has expanded its applications and, by enabling the determination of the position of points on the earth's surface with sufficient accuracy for geodetic surveys, has attracted the interest of topographers, who have contributed to developing new positioning solutions.

As a further development of satellite navigation systems, the *Global Navigation Satellite System* (GNSS) was simplified to set up suitable infrastructures for wide-ranging Earth

monitoring for scientists all over the world. As widely known, four satellite navigation systems will be fully operational in 2023, e.g., the American Navstar GPS [2], the European Galileo system [3], the Russian GLONASS system [4], and last but not least, the Chinese BeiDou Navigation Satellite System (BDS) [5]. In the next few years, other three GNSS systems will be available: those defined as Regional Navigation Satellite Systems (RNSS), including the Japanese Quasi-Zenith Satellite System (QZSS) [6], the Regional South Korean Positioning System (KPS) [7], and the Indian Regional Navigation Satellite System IRNSS/NavIC [8].

The large amount of data provided by GNSS systems contributed to the development of hardware and software such as those of Continuously Operating Reference Stations (CORS), which allows research bodies and technicians to acquire free data at global, national, and regional scales. Moreover, according to the upcoming CORS upgrades to four constellations currently operational (GPS, Galileo, GLONASS, and Beidou), these systems can provide enormous full-scale potential for both scientific and technical augmentations [9].

According to Anderson et al. [10], CORS are crucial in the creation, characterization, and functionality of the National Spatial Reference System (NSRS). Nations' future positioning-related endeavours rely on the correct application of CORS technology. Consequently, the national geodetic survey (NGS) is tasked with ensuring that the national CORS system is resilient, sustainable, and capable of catering to the diverse needs of the geospatial user community. Site monumentation is a critical component of CORS, requiring both significant positional stability and a minimal environmental impact on GNSS signals. The deployment of the national CORS network necessitates collaboration among numerous organizations. Hence, monument materials should be easily obtainable, installation procedures should be uncomplicated, and overall costs should be economical.

The importance of CORS is not only related to geodetic and topographic applications. Indeed, as an example, the Australian *Department of Industry, Innovation, Climate Change, Science, Research, and Tertiary Education* (DIICSRTE) has verified that the placement of CORS networks is capable of increasing the economic benefits of an entire nation, depending also on the Gross Domestic Product (GDP); the estimated increase in Australia's is from $2.3 and $3.7 billion in the year 2012 to $7.8 and $13.7 billion more recently in 2020 [11].

On the other hand, scientific studies concerning GNSS CORS are very extensive and cover many fields of research; therefore, a detailed and systematic review of all the CORS topics appears not to be developable within a single paper. This work proposes a selected review of some applications in the field of GNSS CORS, including *network monitoring, reference frame, structure monitoring, and reachable accuracy*, within which the University of Palermo (Italy) has conducted some experiences over the last 10–15 years. The review is structured as follows: in Section 2, the literature review and state of the art are discussed, including the main studies on the GNSS CORS network; in Section 3, the results obtained from UNIPA GNSS CORS are reported. Finally, Section 4 provides some concluding remarks and possible developments of the research.

2. Literature Background

2.1. Systematic Review Process

For the systematic review of the literature, a formalized process was adapted from [12–14].

Once the research topics were established, a review protocol was established that encompassed the preliminary stages of the literature analysis, including: (i) designing the search strategy and the literature resources; (ii) establishing the selection criteria.

Designing the inclusion and exclusion criteria to be used on certain literature resources is the initial step in selecting candidate papers that could provide valuable insights to address the research questions.

The search strategy has been structured for an objective bibliographic search, although it of course preserves some level of subjectivity. Various keywords, improperly employed as synonyms for research purposes, can be chosen when querying a database (mutually

inclusive keys), or the search might encompass mutually exclusive keys. The investigation can be limited to a timeframe that is assumed to be relevant to the scientific progression of a research topic. The query might also be associated with one or more scientific-disciplinary fields, or it may exclude certain areas.

While there may be some overlap in the query of different research topics, the importance of tailoring the search on a database to the specific topic at hand.

Intending to objectify the research, we made some choices in Scopus "Advanced Query". The search has been executed solely on: (i) the "Title" field (query TITLE in Scopus); (ii) both the "Title" and "Abstract" fields combined (query TITLE-ABS in Scopus). Keywords such as GLONASS, GPS, GNSS, GALILEO, and BEIDOU were used as mutually exclusive, analogously CORS and PERMANENT keywords. The search has been limited to some subject areas of physical sciences (query SUBJAREA in Scopus), namely: engineering (ENGI), earth and planetary sciences (EART), physics and astronomy (PHYS), computer science (COMP), and environmental science (ENVI).

Specific keys have been added for searching specific research topics; for instance, DESIGN or PROJECT keywords were used as mutually exclusive to select candidate papers concerning network design, while ACCURACY and PRECISION mutually exclusive keywords were added for selecting the literature on accuracy assessment.

Once the search keys were identified, in this manuscript, the search was conducted using the Scopus database only. After a subset of manuscripts have been selected, they can be examined based on the number of citations, the publication date, or in connection with the most prolific author in that research field. It's implicitly assumed that manuscripts with a high citation count have significantly influenced the particular research topic. However, the most groundbreaking developments might be discovered in papers that have been recently published but have yet to receive many citations.

The query of a database can vary depending on the research topic. For instance, when conducting a database search on the design of GNSS networks, the search keywords employed might differ from those used when searching for applications for monitoring a structure.

An initial query gave an indication of the trend in the number of publications in GNSS CORS (Figure 1). The query was based on both title and abstract, using the keywords GLONASS, GPS, GNSS, GALILEO, and BEIDOU as mutually exclusive and limiting the results to some subject areas of physical sciences (engineering, earth and planetary sciences, physics and astronomy, computer science, and environmental science).

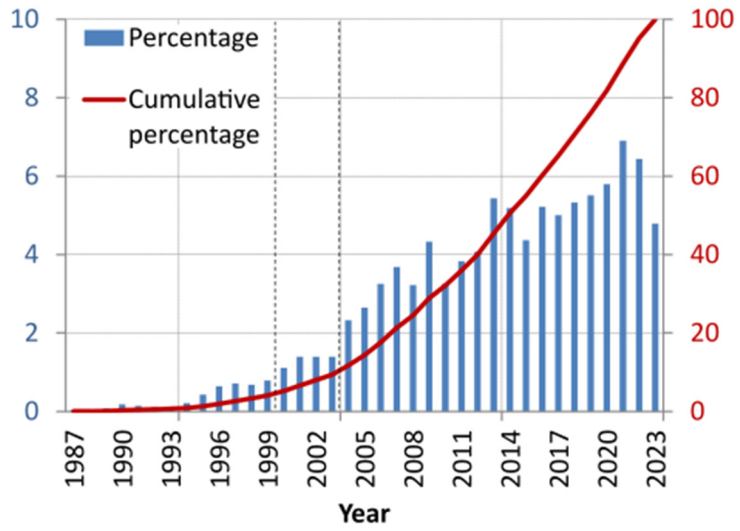

Figure 1. Percentage of GNSS CORS publications (blue bars, primary y-axis) and cumulative percentage (red line, secondary y-axis) from 1987.

Results indicated a change in the trend in the number of publications in the years 2000–2003 (dashed lines). Therefore, it was chosen to limit the query to the period from the 2000s to the current year.

Considering the previously mentioned constraints, the analysis focused on the most frequently cited articles, those we deemed innovative, or some published by particularly active research groups in selected GNSS CORS research areas. These areas include network monitoring, reference frames, structure monitoring, and achievable accuracy.

2.2. Background Articles on GNSS-CORS Network Monitoring

Many works deal with the theoretical network monitoring of CORS; indeed, numerous studies have been developed following the guidance on implementation, materialisation, and executive design by *Anderson* et al. [10]. The *MultiRef* approach (Fortes et al. and Pugliano and Lachapelle [15,16]) was investigated to analyse the influence of the network geometry design on the obtainable accuracy. These analyses showed that the best results are gained when reference stations are distributed at a regular distance; furthermore, CORS stations located outside the study area do not significantly increase accuracy [16]. Two papers by Grejner-Brzezinska et al. discuss the stations' separation, the effects of CORS geometry, and the data reduction technique on the reliability of the rover positioning solution considering that of the Ohio CORS [17,18]. *Kenyeres and Bruyninx* identified the main factors affecting the quality of coordinates' time series in the EPN (EUREF Permanent Network) in Europe, installed for reference frame maintenance [19]. Soler et al., Stone, Snay, and Soler analysed the *Online Positioning User Service* (OPUS), a full Web-based software that processes GPS observation from the United States Department of Commerce's *National Geodetic Survey* (NGS) CORS network, bringing almost 200 organisations together at various levels: academics, private sector, and also governmental [20–22]. Among the most cited articles, there are the experiences of Rizos and Satirapod and Mekik et al.; the first author describes the context in which the Global Geodetic Observing System (GGOS) was established, discussing the role of GPS/GNSS network infrastructure in the implementation of the GGOS mission and providing an update status in Thailand of GNSS CORS [23]; the second paper discusses the infrastructure of the Turkish RTK CORS Network denominated Türkiye Ulusal Sabit GNSS Ağı—Aktif (TUSAGA-Aktif) [24].

Of particular significance in the literature is the work of Odijk et al. that studied real-time kinematic precise point positioning (PPP-RTK) with centimetric precision employing the Perth GPS Network regional CORS [25], while Li and Teunissen studied the benefits of array-assisted CORS ambiguity resolution [26].

In more recent years, the efforts of scientists in the design of GNSS CORS have explored the applicability of these services to wide-area satellite navigation systems. Liu et al., for instance, reported their experience in the People Republic of China on the use of ground-based augmentation systems (GAS) using the BeiDou global navigation satellite system (BDS-3). Many tests have been conducted on the performance of the GAS service, showing its suitability for positioning at different levels of accuracy [27].

Another recent study, carried out in Asia by Gond et al., discussed the contribution of CORS to a long-standing issue in India, in particular regarding the transport infrastructures and their mapping. In this regard, the Indian mapping agency *Survey of India* (SOI) is deploying a CORS network to improve the precision of three-dimensional positions obtained via GNSS [28].

Analogously, in Egypt, the *Egyptian Surveying Authority* (ESA) has established a CORS network consisting of more than 40 stations covering the Nile valley and its delta to assess the quality of ESA-CORS data to monitor tectonic movements. The study analyses the reliability of free Canadian Spatial Reference System Precise Point Positioning (CSRS-PPP) software over more than 30 ESA-CORS claiming millimetric accuracy [29].

The augmentation of the GNSS CORS network has been crucial in providing continuous positioning in various scientific areas. However, gaps in the system, interference from

buildings and vegetation, and problems in deep mining pits and underground mines limit the possibility of using augmented GNSS CORS in all situations.

The topics of *radio frequency interference* (RFI), multipath, and quality control of data from GNSS permanent station networks represent well-established issues, having been studied and analysed in the literature in several cases in recent years. It is hardly worth mentioning that the sources of interference with GNSS signals can be military, microwave, and telecommunication-related transmissions close to the typical L1 band, while amateur radio links can cause disruptions in satellite reception close to the L2 frequency.

Teferle et al. showed how GNSS permanent stations can be affected by both RFI and multipath phenomena; by using electromagnetic spectrum analyzers and wide-band antennas, it is also possible to know the position of the interference source [30]. The software tools used to represent the data in this study are mainly TEQC by Estey and Meertens [31], Generic Mapping Tools, and GMT by Wessel and Smith [32].

Bhatti et al. describe the theoretical treatment of RFIs concerning the signal coming from the GNSS and report a possible solution through a direct system of frequency sensors that simultaneously detects several sources of interference [33]. Several electromagnetic sources, indeed, could degrade the performance of GNSS CORS receivers, and their effects can be both in the band and in the secondary harmonic series generated by transmitters of other communication systems due to non-linear or out-of-band distortions through signals that occupy frequency band widths very close to the GNSS bands. Motella et al., for example, through an analysis with automatic gain control (AGC, used also by Akos), found that digital/analogue TV broadcasts represent a potential source of interference for GNSS applications on a dataset of the city of Turin (Italy) [34,35]. Many authors have proposed studies on RFIs related to GNSS CORS, and in particular some of scientific interest: Jada et al. regarding the aircraft receiver [36], Hu et al. in the field of technology, Auto-Steering Guidance of Agricultural Machinery [37], and last but not least, Barr et al. investigating the performance of multi-beacon DGPS [38].

More recently, Morrison et al. reported that a European RFI monitoring system covered all GNSS bands with a focus on Galileo's E6 L-band, while Miguel et al. developed a low-cost GNSS RFI monitoring system that can be used to detect urban RFIs [39,40].

2.3. Background Articles on Reference Frames and Structure Monitoring

Before delving into this section, it's crucial to highlight the comprehensive review conducted by Bock and Melgar on the physical applications of GPS CORS. This work begins with an overview of GPS, including its constellation and signals, infrastructure, surveys, and positioning methods. It then thoroughly discusses topics related to space geodesy reference systems, coordinate transformations, and GPS position time series. The review also emphasises other aspects of GPS CORS, such as tectonic and crustal deformation, natural hazard mitigation systems, atmospheric monitoring, and climate [41].

Since their development, the main applications of CORS have concerned reference frame definition and land monitoring (in terms of subsidence, seismology, and volcanology). Kenyeres and Bruyninx investigated the permanent network (EPN) of the Regional Reference Frame Sub-Commission for Europe (EUREF) with reference frame maintenance, analysing the quality of the coordinate time series and the site velocity estimation, involving continent-wide spread CORS [19]. The review by He et al. is also noteworthy, where they assessed the techniques and software packages for optimal noise modelling in GPS CORS time series, along with processing strategies and error mitigation [42].

Soler and Snay also carried out a case study on a new set of parameters (for transforming positional coordinates and velocities) between the International Terrestrial Reference Frame of 2000 (ITRF00) and the North American Datum of 1983 (NAD 83) using CORS data by Natural Resources Canada and the U.S. National Geodetic Survey (NGS) [43]. Regarding the South American subcontinent, the *Sistema de Referencia Geocentrico para las Americas* (SIRGAS) was presented in *Brunini* et al. [44,45]. As is well known, SIRGAS represents the geocentric reference system for the South Americas; its definition is equivalent

to the International Earth Rotation and Reference Systems Service (IERS) International Terrestrial Reference System (ITRS), and it is realised by regional densification of the IERS International Terrestrial Reference Frame (ITRF). In 2018, Wang et al. presented the results of North China Reference Frame 2016 (*NChina16*), which deals with landslides and subsidence using five years of continuous GPS observations from 12 CORS fixed on the North China Craton [46]. Other studies at national or regional scales can be further explored, e.g., those of Rizos and Satirapod about GNSS CORS in Thailand [23], Mekik et al. for the TUSAGA-Aktif Network (Turkish national CORS) [24], Yu and Wang for the geodetic infrastructure in the Gulf of Mexico Region [47], Kearns et al. for a subsidence test area in Houston metropolitan area, Texas, U.S.A. (Houston16) [48] or, also, Vestøl 2011 et al. for the land uplift model NKG2016LU, with a new land model for Finnish-Scandinavia (Fennoscandia) peninsula and the neighbouring Baltic Region [49].

The use of CORS was also aimed at seismic displacement assessment operations, especially in the most geo-seismically active areas around the world, such as the South American plates [50], Chile and Mexico [51], Turkey [52–54], and the USA [55]. Another field of application of CORS concerns the investigation of ground deformations by analysing the estimated time series of velocity fields. Based on the important scientific contribution given to these applications by the review of Herring et al. [56], many other studies have been developed in recent years in different countries, such as the Sierra Nevada (USA) [57], Andes (Chile) [58], Caribbean region [59], Himalaya (India) [60,61], Turkey [62], Greece [63], and the Alpi region (Italy) [64]. It is worth mentioning that CORS were also used in other recent applications concerning tunnelling via BDS [65], bridges [66] and dams [67], monitoring, mining [68], and combining different satellite techniques, such as GNSS and Interferometric Synthetic Aperture Radar (InSAR) [69–71].

2.4. Background Articles on CORS Accuracy

In recent years, the development of information technology (IT) infrastructures related to CORS networks has made possible the investigation of their accuracy for classical topographical applications, of which many works have been mentioned.

Two papers by Teunissen, Odijk, and Zhang et al. represent some CORS research milestones: in the first, Teunissen et al. present the PPP-RTK method based on the non-differentiated GNSS observations studied in Delft in the 1990s on two CORS differing in inter-station distances (Hong Kong CORS Network, 30 km, and GPS Network Perth, 70 km) and the method's performances. In the second paper, analogously, Zhang et al. applied the method to the other two GPS CORS networks with inter-station distances ranging from 60 to 100 km. The tested CORS networks were the northern China network and the Australian Perth network. In the two papers, the fast GPS surveying is based on the *Least-squares AMBiguity Decorrelation Adjustment* (LAMBDA) [72–74].

Furthermore, Eckl et al. reported the processing of ten days of GPS data to investigate the accuracy of a three-dimensional relative position vector between GPS antennas, depending on the chord distance between these antennas [75]; also, Soler et al. describe the accuracy of Online Positioning User Service (OPUS) solutions for short observation sessions (1 to 4-h). Feng and Rizos also describe network-based geometry-free models for three carriers' ambiguity resolution (TCAR) and phase bias estimation with a double-differenced (DD) solution [76]. Most cited articles analysing instead the long inter-distances between the sites of the CORS are published by Eren et al. [77], Li et al. [78], and Dabove et al. [79]. Articles by Schwarz et al. [80] (USA), Aponte et al. [81] and Edwards [82] (United Kingdom, UK), and also Ding et al. [83] (Australia) on the evaluation of the accuracy of nationwide networks are the most widely rated in the literature. Also, the evaluation of CORS accuracy represents one of the main topics analysed in low-cost receivers [84–86] and UAV trajectory [87–89].

As is well known, the accuracy of GNSS CORS is dependent on various aspects, such as RFI or multipath problems. However, there are another series of limitations to the use of data from CORS, which differ in nature and consistency.

Certainly an important role plays in the noise reduction of time series: Williams et al. have since 2004 investigated the influence analysis of the error of continuous GNSS CORS position time series, with lengths of the series ranging from a few months to over 10 years. In particular, using maximum likelihood estimation (MLE), the noise was taken to be only white noise, a combination of white noise plus flicker noise, or a combination of white noise plus random walk noise. All noise components show a latitude addictiveness in their amplitudes (greater in equatorial sites) coupled with a bias towards larger values in the southern hemisphere [90]. Also, Van Dierendonck et al. have addressed the issue of GNSS CORS time series reduction with a performance of Narrow Correlator spacing in the receiver [91]. More recently, Yang et al. carried out methods to determine noises in the GNSS vertical coordinate time series (as the white and flicker noise) using time series from the Crustal Movement Observation Network of China (CMONC). The results show that the average flicker noise in the time series was reduced from 19.90 mm/year $^{0.25}$ to 2.8 mm/year $^{0.25}$ [92].

Also, another limitation was the GNSS CORS signal extraction: Sun et al. propose new strategies to detect spoofing attacks on GNSS signals through a signal quality monitoring (SQM) technique [93], while Andreotti et al. investigate an analysis of signal propagation and signature extraction for GNSS indoor positioning [94].

The massive amount of data available from GNSS CORS has allowed an accurate and thorough evaluation of the influence of effects correction, specifically the troposphere and ionosphere ones. For instance, Zhao et al. proposed a new algorithm for troposphere tomography using a truncation factor model (TFM) to solve the sectional slant of water vapour within the tomographic area [95]. On the other hand, Tsugawa et al. using data from three different CORS, analysed the large-scale travelling ionospheric disturbances (LSTIDs) during a geomagnetic storm using Total Electron Content (TEC) [96]. Meanwhile, Komjathy et al. estimated the inter-frequency biases of satellites and receivers and the total electron content (TEC) of the ionosphere among 1000 available CORS using an algorithm developed at the Jet Propulsion Laboratory (JPL), based on the Global Ionospheric Mapping (GIM) software [97]. Wielgosz et al. evaluated the influence of the correction accuracy on-the-fly (OTF) ambiguity resolution (AR) in long-range RTK GPS on instantaneous (single-epoch) ARvand; the results proposed that the correction accuracy deteriorates to the point (during a strong ionospheric storm) that OTF AR takes much longer to fix integers [98]. Lee et al. discussed comparisons of ionosphere database analyses post-processed for the Wide Area Augmentation System (WAAS) with Jet Propulsion Laboratory (JPL) data from the CORS database [99]. Hong et al. also proposed a specific algorithm that uses the geometric conditions between satellites and tracking receivers to determine the differential code bias (DCB) of receivers using CORS stations. This method can be used to estimate the DCBs of receivers in a regional network, as long as one of the DCBs of the receivers is known and therefore does not require a traditional ionosphere model [100]. In 2011, Ji et al. and, more recently, Zhang et al. (2021) studied the slant TEC (STEC) observations of local CORS: in the first paper, the Equatorial ionospheric zonal drift was analysed; in the latter, using a newly defined Modified PPP (MPPP) model, the degradation of PPP performance and the temporal variations of the receiver code biases were estimated; also, their negative impacts on PPP parameters were mitigated, such as ionospheric delays, ambiguity parameters, or receiver clock offsets [101,102].

Last, Xiao et al. using the neural network algorithm, determined a newly modelled Zenith tropospheric delay (ZTD) for high-precision positioning by CORS [103], while Graffigna et al., studying ZTD with the effects that a hurricane had on spatial and temporal behaviour, showed that the ZTD time series exhibited a rapid increase of more than 10 cm in a few hours when the study area was inundated by the hurricane [104].

3. Discussion

Beyond the research on positioning accuracy, given its versatility, the potentiality of UNIPA GNSS CORS positioning has been tested on a wide range of applications, including network monitoring, and accuracy, as mentioned in the introduction.

3.1. The UNIPA GNSS CORS Network Monitoring

With an area of 25,711 km^2, Sicily (Italy, Europe) is the largest island in the Mediterranean Sea and occupies a strategic position that has made it, over the centuries, a centre of attraction and a crossroads of people and artistic, cultural, and scientific traditions. Until the last decade, the presence of GNSS CORS was limited exclusively to deformation monitoring and strain control activities. Two main CORS networks managed by the INGV (*Istituto Nazionale di Geofisica e Vulcanologia*, Italian National Institute of Geophysics and Volcanology) and the Italian Institute for Environmental Protection and Research (*Istituto Superiore per la Protezione e la Ricerca Ambientale*, ISPRA) have been implemented in the last decades.

In Sicily, the INGV integrated network, named *RING,* has been located in the most seismogenetically relevant areas of the eastern part of the island [105,106], due to the presence of Mount Etna volcano and with higher seismological interest. More generally, this network consists of about 200 stations located throughout Italy, and it is one of the most important CORS networks in Europe and the world. Differently from the RING, another GPS network, called *SiOrNet,* was aimed at monitoring deformation cycles along some faults belonging to the oriental coast of Catania (Timpe) [107]. The *SiOrNet* GPS network was located in a more restricted area around the Acicatena and S. Tecla-Linera faults (Catania). This network provided valuable support to ISPRA after the volcanic and tectonic events of Etna in 2002 and is a helpful addition to the *Ithaca project* database. Since 2008, the *UNIPA GNSS CORS* public network (Figure 2) has been developed and implemented by researchers at the University of Palermo, with Topcon instrumentation, in the framework of the national research project *PRIN2005* (Networks of GPS permanent stations for real-time surveying).

It consists of nine permanent stations (SPs), framed in the RDN (*Rete Dinamica Nazionale*, powered by IGM) ETRF2000 datum, and managed by Geo++ software version 2004 and Nearest (Near), *Flächen Korrektur Parameter* (FKP), and Virtual Reference Station (VRS) streams [108].

Topcon Positioning Italy (TPI) as a commercial activity and as a result of the collaboration with the university has then expanded the network by installing additional stations in the eastern part of Sicily; thus, nowadays, the network has 17 SPs, framed in the IGS05 datum, managed by Geo++ software version 2004, with VRS and Near available streams. TPI has managed all CORS on the Topcon Live network since 2012 [109].

The papers of Dardanelli et al. [108–110] showed all details concerning the *UNIPA GNSS CORS* network design, preliminary analyses with statistical analysis, data availability, and the used geodetic framework, with the coordinates, time series, and displacements from 2008–2012. Table 1 shows the coordinates of the *UNIPA GNSS CORS*.

During the first design phase, an RFI was the subject of study regarding the CORS in Palermo, and the radio frequency interferences (RFI) affecting the CORS activities were verified in another application of research [110] through electromagnetic field measurements and GNSS analyses with scientific software (TEQC by UNAVCO, QC2SKY by the Polytechnic of Turin, and Network Deformation Analysis (NDA) by Galileian Plus) to evaluate RFI influences on tropospheric and ionospheric models.

Specifically, the RFI on the Palermo permanent station was analysed during the period 2007–2008. In 2006, three weeks of preliminary electromagnetic monitoring were conducted with a PMM 8055 before permanent stations started their monitoring activities. In particular, the permanent station is equipped with a Net-G3 Topcon receiver using double GPS/GLONASS constellations, is Galileo-ready, and is placed in a plastic rack on a building.

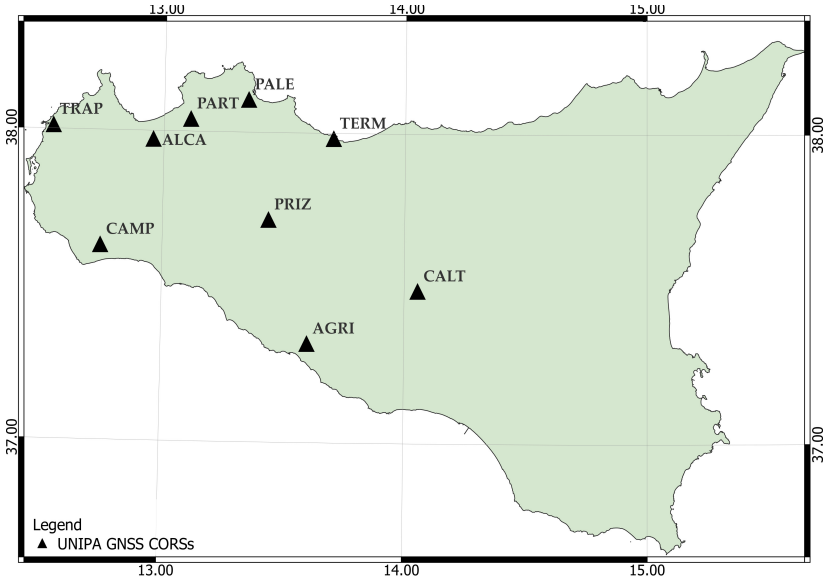

Figure 2. Location of the first group of the UNIPA GNSS CORS [103] in Sicily (Geocentric CRS RDN2008–EPSG: 6706). Geodetic positions in the ETRF2000 and IGb08 systems are shown in Table 1.

Table 1. UNIPA CORS geocentric coordinates in ETRF2000 and IGb08 systems.

CORS	ETRF2000 Epoch 2008.0			IGb08 Epoch 2008.0		
	X (m)	Y (m)	Z (m)	X (m)	Y (m)	Z (m)
AGRI	4,936,331.298	1,194,330.469	3,845,900.834	4,936,330.975	1,194,330.805	3,845,901.113
ALCA	4,906,356.920	1,128,732.790	3,903,344.287	4,906,356.527	1,128,733.024	3,903,344.578
CALT	4,915,665.644	1,230,635.292	3,861,348.275	4,915,665.317	1,230,635.627	3,861,348.553
CAMP	4,933,161.054	1,115,797.238	3,873,024.868	4,933,160.640	1,115,797.477	3,873,025.139
PALE	4,889,534.473	1,160,203.648	3,914,738.514	4,889,534.164	1,160,203.926	3,914,738.891
PART	4,898,768.970	1,140,862.867	3,909,130.415	4,898,768.541	1,140,863.11	3,909,130.693
PRIZ	4,914,033.464	1,174,031.855	3,881,405.827	4,914,033.044	1,174,032.102	3,881,406.106
TERM	4,890,361.337	1,192,337.028	3,904,013.032	4,890,360.965	1,192,337.292	3,904,013.365
TRAP	4,911,563.389	1,092,566.455	3,906,585.782	4,911,562.977	1,092,566.697	3,906,586.062

Although fearing RFI by GSM repeaters was placed on surrounding buildings less than a kilometre away from the roof, results did not show electromagnetic fields that could interfere with GPS. In June 2007, during the first network trials, interferences were detected in the L2 signal. Using an *R&S FSP Spectrum Analyzer* and a *Horn Ets Lindgreen 3115* antenna, electromagnetic signals at L1 and L2 GPS frequencies were spatially explored, searching for the direction of the interfering signal (Figure 3).

The approximate direction of the interfering signal was found, and it was probably of military use for investigative purposes. Data analysis in the graphical representation shows that the first interference occurred from June to August 2007, then became stronger from November 2007 to July 2008, when the signal-to-noise ratio (SNR) was low. Fortunately, the interference did not affect L1 values; multipath values were also high and returned to normal in August 2008. A posteriori data quality control by QC2SKY confirmed the previous conclusions. To obtain a semi-quantitative estimate of the external signal interference on the choke ring antenna placed on the roof, the electromagnetic signal was irradiated with an apparatus consisting of an *R&S SMIQ03B Generator*, an *AR 15SIG3 Amplifier*, and a *Horn Ets Lindgreen 3115* antenna.

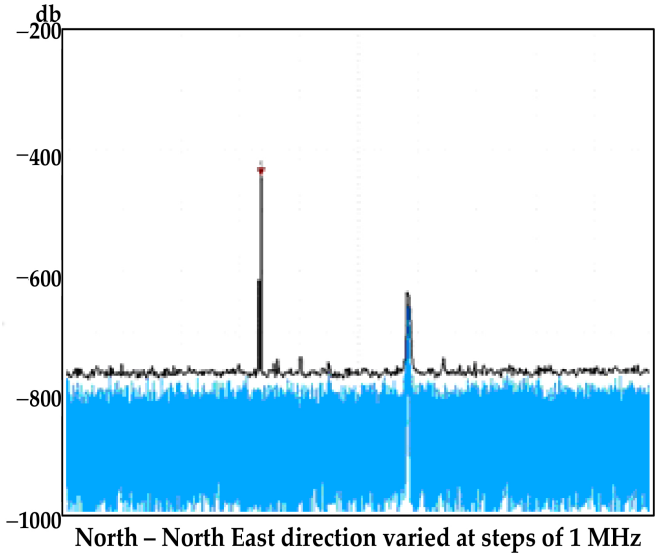

Figure 3. Interference Station Position determination [111].

3.2. Monitoring and Displacements

Since 2014, UNIPA researchers have carried out several studies on dam monitoring, using the Castello Bivona Earth Dam on the Magazzolo reservoir as a case study. The reservoir is located in Sicily and is mainly used for civil purposes, especially for irrigation of agricultural plots during the summer.

The first application was reported in [111]; three GNSS geodetic receivers were installed on the top of the dam, to be used as control points in the sections of the dam most vulnerable to loads. The three receivers were able to transmit data to the department control centre of the University of Palermo via GSM.

The main aim of this work was to test the GNSS post-processing accuracy for the determination of static results compared with other monitoring techniques, such as spirit levelling. Indeed, until today, Italian legislation did not provide for the use of GNSS to manage or monitor dam displacements but only for cadastral surveys. Various static monitoring methods using GNSS can be found in the literature, all of which are related to the fact that the geodetic receiver of the base station is permanently positioned close to the dam, thus not providing a guaranteed accuracy of the results independent of the displacement of the crown (top of the dam). So, in this first paper, a new approach compelling the GNSS receivers has been engaged to sort out these problems. The results obtained using the innovative GNSS approach reveal great performance, and the use of GNSS receivers at different sections of the dam allowed additional information about deformations over time that is not operationally possible to retrieve elsewhere. The post-processing positioning accuracy was approximately a few millimetres, and the results obtained with two different software, *Bernese* (ver. 5.0) and *NDA* (ver. 2009), were comparable in magnitude. As mentioned above, the monitoring of three different sections of the dam revealed different displacements behaviour (in both periodicity and time) that seems to be associated with water depth (and the water surface assessed via remote sensing) (Figure 4).

A few years later, in 2017, the authors showed a comparison between different mathematical models for evaluating the displacements of the earth dam [112]. The mentioned models were hydraulic models, which have already been tested on concrete dams, and finite element models (FEMs), able to engage geotechnical parameters. The results obtained over a period of two years were satisfactory, and the comparison between the models revealed residuals of a few millimetres. Again, results from GNSS monitoring were compared with those obtained from the analysis of hydraulic and finite element methods to determine the most accurate one.

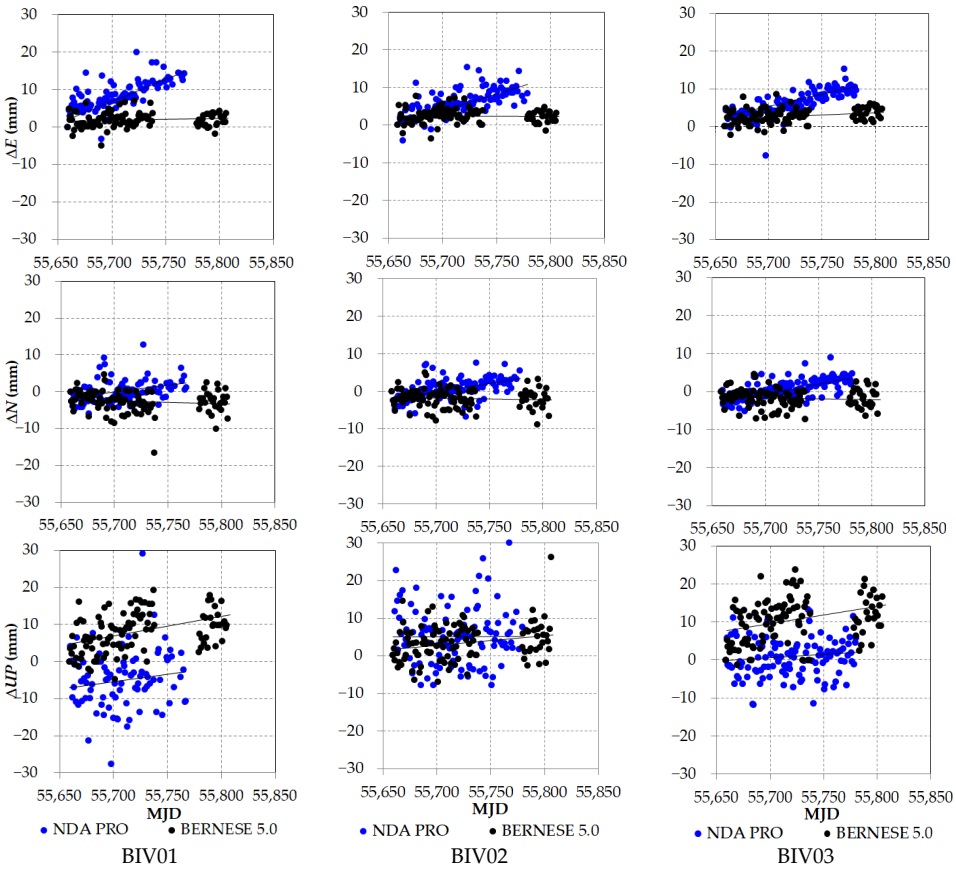

Figure 4. The shift with time of Δ*E*, Δ*N*, and Δ*UP* solutions is estimated via Bernese 5.0 and NDA (blue and black dots, respectively) at the receivers' positions BIV01, BIV02, and BIV03. Adapted from [111].

The results were compared with those obtained with different hydraulic models. Despite being generally referred to as concrete dams, the planimetric components of the displacement by the geotechnical FEM model were similar to those of the deterministic model with millimetre deviations, and in none of the cases, the threshold was higher than 5 mm.

An article testing combined techniques for dam monitoring is, nowadays, one of the most cited in the literature in this field [112]. In this paper, both GNSS and remote sensing techniques were used; the latter, in particular, allowed monitoring of the water level of the reservoir. The water surface was estimated by different approaches, employing both SAR images (TerraSAR-X and Cosmo SkyMed), characterised by different acquisition spectral resolutions, modes, or geometric and optical (ASTER, OLI-TIRS, Landsat 8, Landsat 7 ETM+ SLC-Off, Landsat 5 TM). Two different techniques were tested for each type of image. Both were suitable to quantify the extension of the reservoir surface, as revealed by a discussion with water levels measured on the dam, allowing the extension of water level assessment from Earth Observation to ungauged reservoirs. In addition, the time series of the displacements by GNSS monitoring were compared with remote sensing assessments to discuss a relationship between the orthogonal component of the displacements by GNSS and the estimated water levels by remote sensing and in situ. During the periods of variations in water level, the time series of the displacements of the central section on the dam crest was able to resolve a small range of variability (±2 mm). Also, it was possible to highlight the different behaviour of the dam deformation versus the reservoir water level during the periods of reservoir emptying and filling (Figure 5).

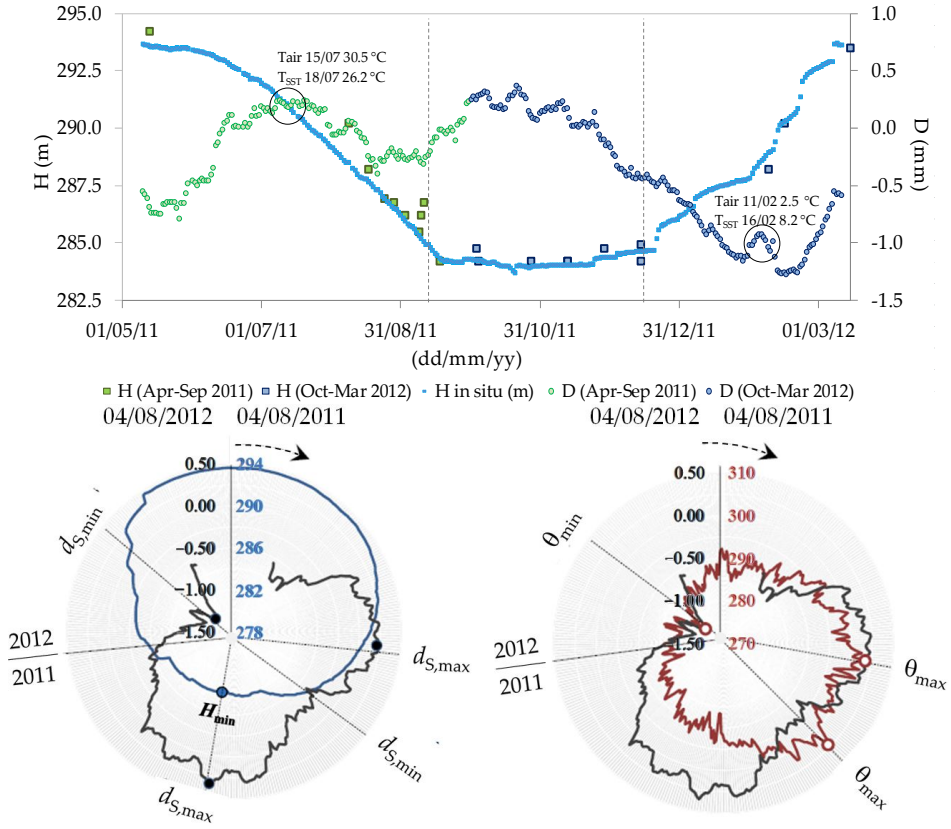

Figure 5. On the top panel: in situ water levels (light blue, primary axis), with superimposed levels estimated from remote sensing during the emptying and filling periods (green and blue circles, respectively), and GNSS-measured displacements (dark blue, secondary axis). On the lower panels: GNSS displacements (d_S, black curve) versus in situ water levels (H, blue curve in the left panel) and versus air temperature (θ, red curve in the right panel).

The behaviour of the displacements with water levels and temperature has led a few years later to further research; in [113] quasi-PS (Persistent Scatter) Interferometric SAR, diachronic thermal analysis and optical-based classification techniques were employed to assess both forcing factors and resulting displacements at the top of the dam over one year. Again, beyond Earth Observation images, including Sentinel-1A interferometric images and Landsat 8 thermal images, the GNSS data were essential to proving the concept. Indeed, the results revealed that it is possible to monitor both temperature-periodic forcing factors and the water levels of the dam and the resulting displacements through the combined use of different remotely sensed data (Figure 6).

Over the years, UNIPA CORS has also been used for geological and geodynamic monitoring and displacement. In [114], an interesting study was presented in which a team of researchers from several international research organisations analysed a stalactite from a karst cave in north-western Sicily (Italy) that provided the first evidence for numerous marine inundations associated with relative sea-level high-stand during the past Middle Pleistocene Transition. The speleothem is approximately a hundred metres above mean sea level because of quaternary uplift.

Three marine hiatuses and a coral overgrowth indicate the age of the final marine ingression, making the speleothem the oldest stalactite with marine hiatuses investigated. By integrating the coral-constrained depth with the geologically constrained uplift rate and making a probabilistic assessment, it was found that the age of the last marine ingression likely corresponds with a marine isotope stage.

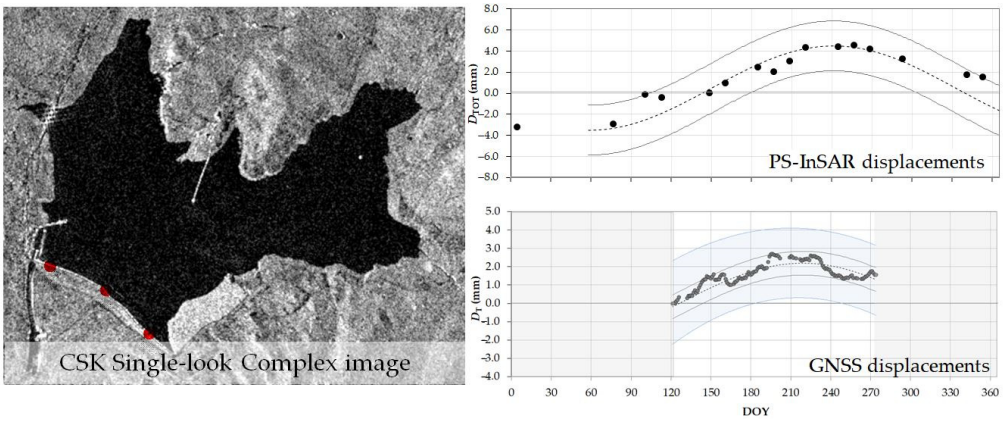

Figure 6. On the left panel: a CSK Single-Look Complex image of the dam-reservoir system. Superimposed the positions of the GNSS receivers (red points). On the right panels: PS-InSAR and GNSS estimations (red dots in the upper right panel and black dots in the lower right panel) of the horizontal total displacements orthogonal to the dam temporal. Superimposed in both right panels, to facilitate the phenomenon comprehension, are a sinusoidal interpolation curve and a confidence band twice the standard deviation between interpolated and in situ values. Adapted from [113].

In this analysis, the orthometric height of the stalactite is determined because of two integrated geodetic survey techniques: GNSS positioning and tacheometric levelling. The static GNSS survey was conducted at several control points near the NRTK over an observation time of 4 h for each point and a 10 km baseline distance. The data were referred to the permanent station of Trapani (TRAP) of the UNIPA NRTK GNSS network. The backward intersection method was used to link the survey inside the cave with the GNSS survey.

Another geological and geodynamics study, presented in a recent paper [115], employed a multidisciplinary approach to detect active geological structures with GNSS static analyses, both onshore and offshore, tectonostratigraphic and morphotectonic.

The test area was selected between the two cities of Termini Imerese and Palermo (in the Apennine-Maghrebian fold and accommodating the Africa-Europe plate convergence). The multidisciplinary approach resulted in the quantification of the relative GNSS velocity field, a new morphotectonic map, a morphotectonic evolution model of the study area, the slip rate of a segment of the westernmost of the two detected faults, a new active tectonic deformation in this region, and a new 3D modelling of two NNW-trending active faults.

In the research [116], by employing static positioning and precise point positioning (PPP), 5-year-long time series of *UNIPA GNSS CORS* were analysed, and a linear trend for all CORS time series was shown with its geodynamic implications.

The last multidisciplinary research resulted in the integration of GNSS and InSAR (interferometric synthetic aperture radar) data [117]. Combined investigations discovered the potential seismogenic sources of destructive earthquakes documented in south-western Sicily. The approach was aimed at estimating the current deformation rate in south-western Sicily and enhancing knowledge about the seismic potential of this area.

Besides proving the versatility of CORS on a wide range of topics, several tests on the accuracy reachable by GNSS were carried out.

3.3. Application for Positioning Accuracy

Mobile Mapping System (MMS) [118,119] presents an additional area of research; then, these points were positioned in NRTK mode. MMS acquisitions were experimented with, enabling the retrieval of terrain morphology, building conditions, footpaths, and street pathways. The initial phase involved surveying numerous benchmark control points in NRTK mode once these were established across the site using static GNSS mode. During the survey, the Leica CS-10 receiver obtained real-time corrections from the GNSS CORS network. The subsequent phase involved an EGNOS-mode survey of the tree species.

Similar to the NRTK survey, numerous benchmarks were initially established in static mode using GPS. These measurements were conducted using a PDA GeoXH Trimble equipped with an optional Zephyr external antenna. In the final phase, the survey was executed using Topcon's IP-S2 MMS. The Spatial Factory software supplied the point cloud gathered by the laser scanner during the survey campaign, the vehicle's plotted trajectory, and spherical images from a 360° camera. For more details, please refer to paper [120].

A new approach was developed to optimise the sampling area across an old-growth forest using geomatics techniques such as GNSS, UAV-borne laser scanning, and radial surveying. This enabled the estimation of structural attributes with tolerable error [121]. The plot size was estimated by visualising the semivariogram of a canopy height model (CHM) by UAV laser scanning. The tree heights estimated by UAV laser scanning resulted in a strong correlation with the heights of the trees measured in situ. However, the positioning of several trees required the use of both GNSS and total station geomatics surveys. Due to the tree heights hindering the GNSS signal transmission, only the GLONASS satellite constellation (which showed the highest dilution of precision during the survey) was used to fix the solution, while the GPS satellite constellation was used to augment position accuracy (PDOP~5−10) (Figure 7).

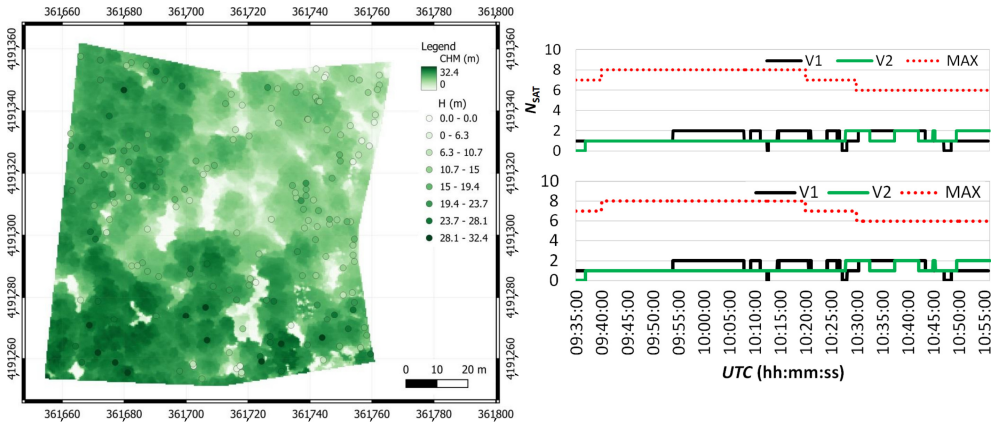

Figure 7. On the left panel: a pseudo-coloured canopy height model with over-imposed trees' heights represented with the same white-green palette. On the right panel, the number of GLONASS and GPS satellites, V1 and V2, are represented with black lines and green lines, respectively. The maximum number of satellites is represented by a dashed red line. Adapted from [121].

As a final highlight of the *UNIPA GNSS CORS* network applications, one aspect is analysed that plays a very interesting role in the accuracy of the network achieved during surveys.

In the paper [122], the advantage of using the multi-GNSS PPP technique in static mode was analysed. Specifically, the main aim of the study was to determine the contribution of the new Galileo satellite system when it is used in addition to those already well-established, such as Navistar GPS and GLONASS. For this purpose, the open-source RTKLib software (version 2.4.2 p13) was used; the dataset available in this work was augmented with satellite precise orbits and clocks from *Collecte Localization Satellites* (CLS) analysis centres for the International GNSS Service (IGS) and *Centre National d'Etudes Spatiales* (CNES). Specifically, the well-known models *Iono-free* (ionospheric errors) and *GOT-4.7* (tidal effects) were used. Two different tropospheric models were also tested: *Estimate Zenith Tropospheric Delay* (ZTD) and *Saastamoinen* models.

Two datasets of 31 and 10 days from a GNSS CORS station located in Palermo and from a benchmark neighbouring the CORS were used and then managed by open-source software for geomatics applications. Seven GNSS configurations were considered: first the three constellation pairs (GPS + GLONASS + Galileo), then the two-and-two pairs (GPS + GLONASS, GPS + Galileo, GLONASS + Galileo), and finally the single pair (GPS, GLONASS, Galileo).

The results (Table 2) showed a significant improvement in accuracy when using the *Estimated Zenith Tropospheric Delay* model compared to the *Saastamoinen* model (the average standard deviation by applying the ZTD was approximately one-third that achieved by applying the Saastamoinen model); also, estimates using combinations of GNSS constellations (in particular GPS+Galileo with the ZTD estimate) performed more accurately than single constellations.

Table 2. East, North, and Up standard deviation, σ, of the ZTD, by employing two different tropospheric models (Estimated Zenith Tropospheric Delay and Saastamoinen) for a given satellite constellation (GPS, GLONASS, Galileo) and their combinations. Values are pseudo-coloured using a green-white-red palette to highlight the models' performances (adapted from [122]).

GNSS Constellation(s)	Estimated ZTD			Saastamoinen Model		
	σ_{East} (m)	σ_{North} (m)	σ_{Up} (m)	σ_{East} (m)	σ_{North} (m)	σ_{Up} (m)
GPS	23	27	38	74	33	60
GLONASS	28	24	11	87	29	60
Galileo	30	29	16	101	51	67
GPS + GLONASS	25	10	10	69	17	55
GPS + Galileo	10	10	6	160	40	63
GLONASS + Galileo	33	26	23	77	28	59
GPS + GLONASS + Galileo	30	17	13	74	22	68

Subsequently, many authors focused on the effects that differential NRTK corrections, with respect to CORS network geometry, can have on GNSS solutions [123] by testing different network configurations and inter-distances between CORS stations (Figure 8).

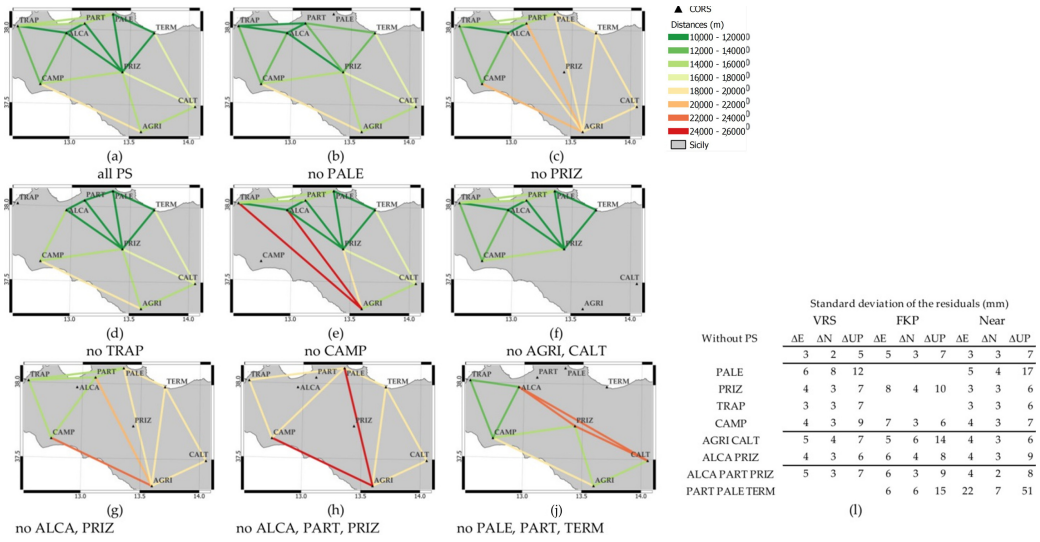

	VRS			FKP			Near		
Without PS	ΔE	ΔN	ΔUP	ΔE	ΔN	ΔUP	ΔE	ΔN	ΔUP
	3	2	5	5	3	7	3	3	7
PALE	6	8	12				5	4	17
PRIZ	4	3	7	8	4	10	3	3	6
TRAP	3	3	7				3	3	6
CAMP	4	3	9	7	3	6	4	3	7
AGRI CALT	5	4	7	5	6	14	4	3	6
ALCA PRIZ	4	3	6	6	4	8	4	3	9
ALCA PART PRIZ	5	3	7	6	3	9	4	2	8
PART PALE TERM				6	6	15	22	7	51

Figure 8. Screenshot of UNIPA CORS geometry. Distances are represented through a green, red, and yellow colour palette for increasing distances, representing the whole network (**a**) or by deactivating 1 PS (**b**–**e**), 2 PSs (**f**,**g**), or 3 selected PSs (**h**,**j**). The standard deviation of the residuals for each network solution is also reported (**l**). Adapted from [123].

A stable pillar benchmark on the top of the *Department of Engineering* was used to perform several tests in static positioning with a dataset of over 40 h of acquisition time. Different geometric schemes were used in this study, evaluating the position that the benchmark could have with regard to the different arrangements (inside the network, outside, and near). Data processing was conducted using alternative network solutions, including Near (closest), FKP, and VRS. The results established the high reliability of the GNSS network, with centimetre accuracy in terms of planimetric coordinates and ellipsoid heights. In terms of the standard deviation of the residuals, results were similar without distinction between the method of correction used and the surveyed network design. Of course, the lower standard deviation of residuals characterised the full CORS network

(~4 mm, on average), similar values characterised the CORS without one or two permanent stations (~5−6 mm, on average), and the worst values obtained by deactivating three permanent stations (~11−12 mm, on average). Considering the network solutions, the best standard deviation of the residuals was obtained on average by applying the VRS (≈5.1 mm), then the FKP (≈6.7 mm), and the Near (≈7.4 mm).

Also, an evaluation of the accuracy of different GNSS geodetic receivers was made, with accuracy used for mapping and guidance of agricultural machines in precision farming [124]. *Quanum GPS Logger V2*, *Thales MobileMapper Pro*, *Stonex S5*, and *Stonex S7-G* were used in this application. Several tests were carried out, including the evaluation of the distance of some points with respect to the NRTK trajectory; the use of differential correction data and an external antenna, demonstrating that the use of an external antenna always improves positioning accuracy; and the satellite receiver, which showed the worst positioning accuracy; the low-cost receiver surprisingly showed a low positioning error (≅0.5 m), used in precision farming.

The evaluation of the coordinates from a GNSS survey (static mode, PPP, or Network Real Time Kinematic) has been investigated in numerous technical and scientific papers. Many of these have been carried out to relate Network Real Time Kinematic (NRTK), PPP, and static modes solutions, assuming the previous in the literature as the true or most reasonable result.

In the article [125], the above-mentioned GNSS surveying methods were compared in pairs, using some benchmark points, to check the congruence of their solutions. The static and NRTK solutions refer to a local GNSS CORS network's investigation. The NRTK positioning was obtained by different methods (NEA, FKP, and VRS), and the PPP solution was expected by using two different open-source softwares (CSRS-PPP version 2 and RTKLIB version 2.4.2 p13). To test the solutions, a statistical approach was used to check whether the distribution frequencies of the coordinate residuals belong to the normal distribution for all examined pairs. In this case study, the hypothesis of a normal distribution was confirmed, in particular for the NRTK vs. static pair, which seems to achieve the greatest congruence, while pairs involving the PPP approach obtained better congruence with the CSRS than using the RTKLIB (Figure 9).

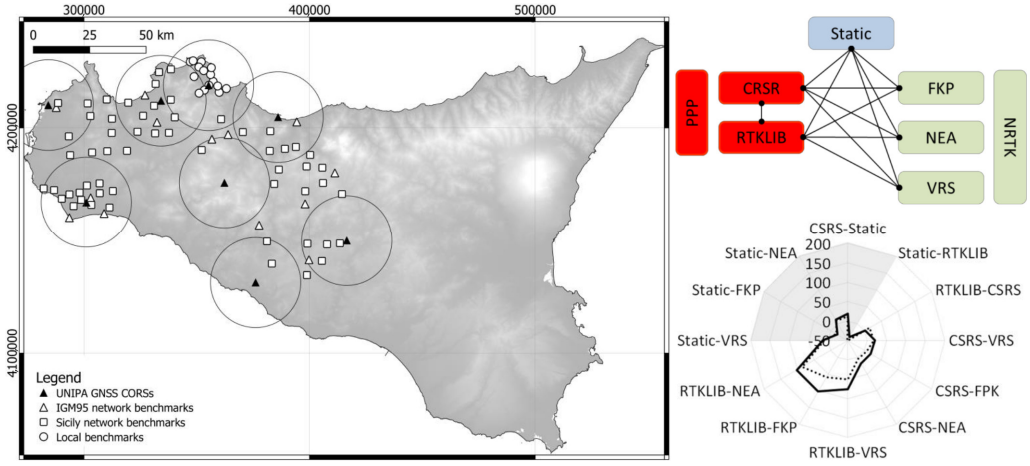

Figure 9. On the left panel, Sicily network benchmarks, IGM95 network benchmarks, UNIPA GNSS CORSs, and local benchmarks are represented with white squares, white triangles, black triangles, and white circles, respectively. Superimposed a 20 km buffer from the GNSS CORS. Reference system: UTM-WGS84 33N (ETRF2000-RDN2008)-EPSG6708. Lower right panel: an example of a spider graph, pre- and post-removal of the outliers (dashed and continuous lines, respectively), for different PPP and NRTK vs. static solutions, with tested pairs reported on the upper right scheme. Adapted from [125].

Finally, Ref. [126], the positional accuracies of some cadastral marks were analysed and compared with official maps produced by Google Earth Maps, local cartography, and the cadastral government department (Figure 10).

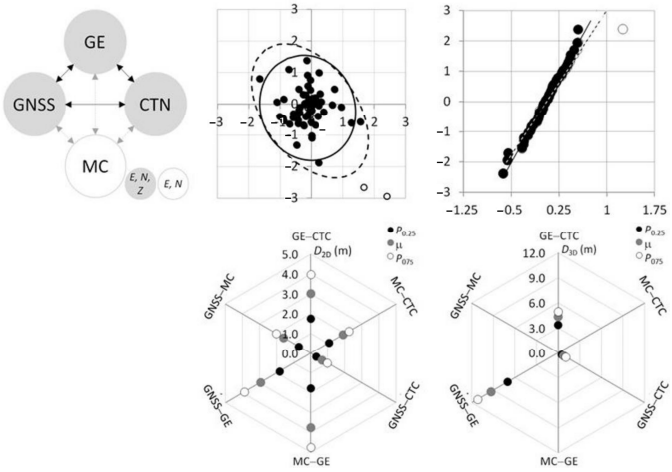

Figure 10. Conceptual scheme of comparisons (top left panel), confidence ellipses pre and post-removal of the outliers (dashed and continuous lines respectively in the upper central panel); pair Q-Q plots for a pair (black dots in the upper right panel, with outliers represented in white); and in the lower panels: I quartile (black dots), average (grey dots), and III quartiles (white dots) of the planimetric and plano-altimetric difference of coordinates of the differences (lower left and right panels, respectively) post outliers removal.

The results showed centimetric accuracy obtained by the GNSS NRTK survey, both in the planimetric and altimetric components.

4. Conclusions and Future Developments

A review of the selected research application, GNSS CORS, has been presented in this paper. Also, 15 years of experience using the GNSS CORS at the University of Palermo (Italy) were briefly reported. For instance, the GNSS CORS has found its applications in many technical and scientific applications, including network monitoring, reference frame, dam monitoring, and the performance of positional accuracy.

Through the growing technical development of fully operational GNSS satellite systems (such as GPS, GLONASS, Galileo, and Beidou), in addition to those that will be implemented in the coming years (such as QZSS, KPS, and IRNSS/NavIC), CORS will be able to receive information from more than 140 satellites simultaneously. This represents an obvious advantage in terms of dilution of precision (DOP), and consequently, it will be easier to avoid electromagnetic interference and benefit from the accuracy.

Several scenarios open up and constitute future fields of exploration for GNSS CORS applications. Among these are new solutions for PPP based on multi-GNSS constellations and their massive use for time series analyses; the validation of reference frames using international GNSS services; the implementation of decision support systems for managing civil infrastructure or urban transport through the integration of GNSS and Earth Observation imaging systems; as well as the use of GNSS and satellite remote sensing techniques for meteorological, climate, and hydroscience studies as hydrogeodesy; the monitoring of ground deformation geohazards; and the monitoring of ionosphere, troposphere, and atmospheric physics through GNSS-R. Finally, the integration of GNSS and InSAR to predict extreme weather events such as drought and flood.

In this scenario of future improvements, however, it is evident that GNSS CORS also has limitations, such as GNSS coordinate time series noise reduction, signal extraction, thermal expansion effect correction, plate motion, common mode error, and so on, which are all important factors affecting the accuracy of GNSS coordinate time series.

At present, the CORS station network and GNSS measurement have been successfully applied to hydrological monitoring, such as the monitoring of land water storage changes and groundwater storage changes.

In the coming years, attention should be turned to other applications, given the wide availability of data collected by CORS. In particular, further interesting applications of satellite navigation by GNSS-R emerging applications could be developed, such as remote sensing techniques of soil moisture content and SmallSats. In addition, GNSS CORS is providing crescent support for several fields of precision farming. The use of GNSS CORS for other hydrology applications could be further developed.

A series of applications could be developed from the potential offered by CORS GNSS data with geographic information system software, such as monitoring electromagnetic fields, the acoustic map of the vehicular traffic of an urban agglomeration, or various environmental parameters, similar to what has been done in previous years [127,128].

Finally, the flexibility of CORS services is opening up new research fields, such as hydrogeodesy, focusing on estimating continental-scale changes in water storage as remotely observed through gravity space missions and regional and local alterations detected using INSAR and GNSS [129].

Author Contributions: Conceptualization C.P. and G.D.; Methodology C.P., A.M., M.L.B. and G.D.; C.P., A.M., M.L.B. and G.D. wrote the original draft preparation; C.P., A.M., M.L.B. and G.D. reviewed and edited the paper. All authors have read and agreed to the published version of the manuscript.

Funding: This research received no external funding.

Data Availability Statement: No new data were created.

Conflicts of Interest: The authors declare no conflict of interest.

References

1. Kissam, P. *Surveying for Civil. Engineers*; McGraw-Hill: New York, NY, USA, 1981; ISBN 978-0-07-034882-0.
2. GPS. Available online: https://www.gps.gov/systems/gps/space (accessed on 22 September 2023).
3. Galileo. Available online: https://www.gsc-europa.eu/system-service-status/constellation-information (accessed on 22 September 2023).
4. GLONASS. Available online: https://www.glonass-iac.ru/en/sostavOG (accessed on 22 September 2023).
5. BDS. Available online: http://www.csno-tarc.cn/en/system/constellation (accessed on 22 September 2023).
6. QZSS. Available online: https://qzss.go.jp/en (accessed on 22 September 2023).
7. KPS. Available online: https://www.gpsworld.com/korea-will-launch-its-own-satellite-positioning-system/ (accessed on 22 September 2023).
8. IRNSS/NavIC. Available online: https://www.isro.gov.in/irnss-programme (accessed on 22 September 2023).
9. Jin, S.; Wang, Q.; Dardanelli, G. A Review on Multi-GNSS for Earth Observation and Emerging Applications. *Remote Sens.* **2022**, *14*, 3930. [CrossRef]
10. Anderson, R.; Chin, M.; Cline, M.; Hoar, D.; Murray, O.; Stone, W. National Continuously Operating Reference Station (National Cors) Site Monumentation. 2000. Available online: https://kb.unavco.org/kb/assets/285/CORS_Monumentation.pdf (accessed on 22 September 2023).
11. ACIL Allen Consulting. The Value of Augmented GNSS in Australia. 2013. Available online: http://www.acilallen.com.au/cms_files/ACIL_GNSS_positioning.pdf (accessed on 22 September 2023).
12. Siemuri, A.; Selvan, K.; Kuusniemi, H.; Valisuo, P.S.; Elmusrati, M.S. A Systematic Review of Machine Learning Techniques for GNSS Use Cases. *IEEE Trans. Aerosp. Electron. Syst.* **2022**, *58*, 5043–5077. [CrossRef]
13. Kitchenham, B. Procedures for Performing Systematic Reviews. 2004. Available online: https://www.inf.ufsc.br/aldo.vw/kitchenham.pdf (accessed on 2 November 2023).
14. Radočaj, D.; Plaščak, I.; Jurišić, M. Global Navigation Satellite Systems as State-of-the-Art Solutions in Precision Agriculture: A Review of Studies Indexed in the Web of Science. *Agriculture* **2023**, *13*, 1417. [CrossRef]
15. Fortes, L.P.; Cannon, M.E.; Lachapelle, G.; Skone, S. Optimizing a network-based RTK method for OTF positioning. *GPS Solut.* **2003**, *7*, 61–73. [CrossRef]
16. Pugliano, G.; Lachapelle, G. La collocazione nel posizionamento GPS network RTK [The least-squares collocation method applied to the network RTK GPS positioning]. *Boll. Di Geod. E Sci. Affin.* **2005**, *64*, 93–106.
17. Grejner-Brzezinska, D.A.; Kashani, I.; Wielgosz, P. On accuracy and reliability of instantaneous network RTK as a function of network geometry, station separation, and data processing strategy. *GPS Solut.* **2005**, *9*, 212–225. [CrossRef]

18. Grejner-Brzezinska, D.A.; Kashani, I.; Wielgosz, P.; Smith, D.A.; Spencer, P.S.J.; Robertson, D.S.; Mader, G.L. Efficiency and reliability of ambiguity resolution in network-based real-time kinematic GPS. *J. Surv. Eng.* **2007**, *133*, 56–65. [CrossRef]
19. Kenyeres, A.; Bruyninx, C. EPN coordinate time series monitoring for reference frame maintenance. *GPS Solut.* **2004**, *8*, 200–209. [CrossRef]
20. Soler, T.; Michalak, P.; Weston, N.D.; Snay, R.A.; Foote, R.H. Accuracy of OPUS solutions for 1- to 4-h observing sessions. *GPS Solut.* **2006**, *10*, 45–55. [CrossRef]
21. Stone, W. The evolution of the national geodetic survey's continuously operating reference station network and online positioning user service. In Proceedings of the 2006 IEEE/ION Position, Location, and Navigation Symposium, Coronado, CA, USA, 25–27 April 2006; Volume 1650658, pp. 653–663.
22. Snay, R.A.; Soler, T. Continuously operating reference station (CORS): History, applications, and future enhancements. *J. Surv. Eng.* **2008**, *134*, 95–104. [CrossRef]
23. Rizos, C.; Satirapod, C. Contribution of GNSS CORS infrastructure to the mission of modern geodesy and status of GNSS CORS in Thailand. *Eng. J.* **2011**, *15*, 25–42. [CrossRef]
24. Mekik, C.; Yildirim, O.; Bakici, S. The Turkish real time kinematic GPS network (TUSAGA-Aktif) infrastructure. *Sci. Res. Essays* **2011**, *6*, 3986–3999.
25. Odijk, D.; Teunissen, P.J.G.; Zhang, B. Single-frequency integer ambiguity resolution enabled GPS precise point positioning. *J. Surv. Eng.* **2012**, *138*, 193–202. [CrossRef]
26. Li, B.; Teunissen, P.J.G. GNSS antenna array-aided CORS ambiguity resolution. *J. Geod.* **2014**, *88*, 363–376. [CrossRef]
27. Liu, C.; Gao, W.; Jiang, L.; Zheng, F.; Lu, J.; Cai, H.; Chen, L. The Development and Performance Assessment of China's CORS. *J. Surv. Eng.* **2023**, *149*, 04023007. [CrossRef]
28. Gond, A.K.; Ohri, A.; Maurya, S.P.; Gaur, S. Accuracy Assessment of Relative GPS as a Function of Distance and Duration for CORS Network. *J. Indian Soc. Remote Sens.* **2023**, *51*, 1267–1277. [CrossRef]
29. Abdallah, A.; Agag, T. Reliability of CSRS-PPP for Validating the Egyptian Geodetic Cors Networks. *Artif. Satell.* **2022**, *57*, 58–76. [CrossRef]
30. Teferle, N.; Bingley, R.; Dodson, A.; Apostolidis, P.; Staton, G. RF Interference and Multipath Effects at Continuous GPS Installations for Long-Term Monitoring of Tide Gauges in UK Harbours. In Proceedings of the 16th International Technical Meeting of the Satellite Division of The Institute of Navigation (ION GPS/GNSS 2003), Portland, OR, USA, 9–12 September 2003.
31. Estey, L.H.; Meertens, C.M. TEQC: The Multi-Purpose Toolkit for GPS/GLONASS Data. *GPS Solut.* **1999**, *3*, 42–49. [CrossRef]
32. Wessel, P.; Smith, W.H.F. A new Version of generic mapping tools released. *EOS Trans. Am. Geophys. Union* **1995**, *79*, 579. [CrossRef]
33. Bhatti, J.A.; Humphreys, T.E.; Ledvina, B.M. Development and demonstration of a TDOA-based GNSS interference signal localization system. In Proceedings of the IEEE/ION Position, Location and Navigation Symposium, Myrtle Beach, SC, USA, 23–26 April 2012; pp. 455–469. [CrossRef]
34. Motella, B.; Pini, M.; Dovis, F. Investigation on the effect of strong out-of-band signals on global navigation satellite systems receivers. *GPS Solut.* **2008**, *12*, 77–86. [CrossRef]
35. Akos, D.M. Who's afraid of the spoofer? GPS/GNSS spoofing detection via automatic gain control (agc). *Navig. J. Inst. Navig.* **2012**, *59*, 281–290. [CrossRef]
36. Jada, S.; Psiaki, M.; Landerkin, S.; Langel, S.; Scholz, A.; Joerger, M. Evaluation of PNT situational awareness algorithms and methods. In Proceedings of the 34th International Technical Meeting of the Satellite Division of the Institute of Navigation, ION GNSS+, St. Louis, MO, USA, 20–24 September 2021; pp. 816–833. [CrossRef]
37. Hu, B.; Wu, C.; Li, J.; Li, X.; Liu, X. Communication Tower Based Experiment and Analysis of Differential Augmentation for Auto-Steering Guidance of Agricultural Machinery. *Lect. Notes Electr. Eng.* **2018**, *497*, 431–441. [CrossRef]
38. Barr, S.P.; Swaszek, P.F.; Hartnett, R.J.; Johnson, G.W. Performance of multi-beacon DGPS. In Proceedings of the International Technical Meeting of The Institute of Navigation, San Diego, CA, USA, 28–30 January 2013; pp. 359–373.
39. Morrison, A.; Sokolova, N.; Gerrard, N.; Rødningsby, A.; Rost, C.; Ruotsalainen, L. Radio-Frequency Interference Considerations for Utility of the Galileo E6 Signal Based on Long-Term Monitoring by ARFIDAAS. *Navig. J. Inst. Navig.* **2023**, *70*, navi.560. [CrossRef]
40. Miguel, N.R.S.; Chen, Y.-H.; Lo, S.; Walter, T.; Akos, D. Calibration of RFI Detection Levels in a Low-Cost GNSS Monitor. In Proceedings of the IEEE/ION Position, Location and Navigation Symposium—PLANS 2023, Monterey, CA, USA, 24–28 April 2023; pp. 520–535.
41. Bock, Y.; Melgar, D. Physical applications of GPS geodesy: A review. *Rep. Prog. Phys.* **2016**, *79*, 106801. [CrossRef]
42. He, X.; Montillet, J.-P.; Fernandes, R.; Bos, M.; Yu, K.; Hua, X.; Jiang, W. Review of current GPS methodologies for producing accurate time series and their error sources. *J. Geodyn.* **2017**, *106*, 12–29. [CrossRef]
43. Soler, T.; Snay, R.A. Transforming positions and velocities between the international terrestrial reference frame of 2000 and North American datum of 1983. *J. Surv. Eng.* **2004**, *130*, 49–55. [CrossRef]
44. Sánchez, L.; Brunini, C. Achievements and challenges of SIRGAS. *Int. Assoc. Geod. Symp.* **2009**, *134*, 161–166.
45. Brunini, C.; Sanchez, L.; Drewes, H.; Costa, S.; Mackern, V.; Martínez, W.; Seemuller, W.; da Silva, A. Improved analysis strategy and accessibility of the SIRGAS reference frame. *Int. Assoc. Geod. Symp.* **2012**, *136*, 3–10.

46. Wang, G.; Bao, Y.; Gan, W.; Geng, J.; Xiao, G.; Shen, J.S. NChina16: A stable geodetic reference frame for geological hazard studies in North China. *J. Geodyn.* **2018**, *115*, 10–22. [CrossRef]
47. Yu, J.; Wang, G. Introduction to the GNSS geodetic infrastructure in the Gulf of Mexico Region. *Surv. Rev.* **2017**, *49*, 51–65. [CrossRef]
48. Kearns, T.J.; Wang, G.; Turco, M.; Welch, J.; Tsibanos, V.; Liu, H. Houston16: A stable geodetic reference frame for subsidence and faulting study in the Houston metropolitan area, Texas, U.S. *Geod. Geodyn.* **2019**, *10*, 382–393. [CrossRef]
49. Vestøl, O.; Ågren, J.; Steffen, H.; Kierulf, H.; Tarasov, L. NKG2016LU: A new land uplift model for Fennoscandia and the Baltic Region. *J. Geod.* **2019**, *93*, 1759–1779. [CrossRef]
50. Sánchez, L.; Seemüller, W.; Drewes, H.; Mateo, L.; González, G.; da Silva, A.; Pampilló, J.; Martínez, W.; Cioce, V.; Cisneros, D.; et al. Long-Term Stability of the SIRGAS Reference Frame and Episodic Station Movements Caused by the Seismic Activity in the SIRGAS Region. *Int. Assoc. Geod. Symp.* **2013**, *138*, 153–161.
51. Sánchez, L.; Drewes, H. Crustal deformation and surface kinematics after the 2010 earthquakes in Latin America. *J. Geodyn.* **2016**, *102*, 1–23. [CrossRef]
52. Uzel, T.; Eren, K.; Gulal, E.; Tiryakioglu, I.; Dindar, A.A.; Yilmaz, H. Monitoring the tectonic plate movements in Turkey based on the national continuous GNSS network. *Arab. J. Geosci.* **2013**, *6*, 3573–3580. [CrossRef]
53. Tiryakioglu, I.; Yigit, C.O.; Yavasoglu, H.; Saka, M.H.; Alkan, R.M. The determination of interseismic, coseismic and postseismic deformations caused by the Gökçeada-Samothraki earthquake (2014, Mw: 6.9) based on GNSS data. *J. Afr. Earth Sci.* **2017**, *133*, 86–94. [CrossRef]
54. Tiryakioğlu, I. Geodetic aspects of the 19 May 2011 Simav earthquake in Turkey. *Geomat. Nat. Hazards Risk* **2015**, *6*, 76–89. [CrossRef]
55. Murray, J.R.; Svarc, J. Global positioning system data collection, processing, and analysis conducted by the U.S. Geological Survey earthquake hazards program. *Seismol. Res. Lett.* **2017**, *88*, 916–925. [CrossRef]
56. Herring, T.A.; Melbourne, T.I.; Murray, M.H.; Floyd, M.A.; Szeliga, W.M.; King, R.W.; Phillips, D.A.; Puskas, C.M.; Santillan, M.; Wang, L. Plate Boundary Observatory and related networks: GPS data analysis methods and geodetic products. *Rev. Geophys.* **2016**, *54*, 759–808. [CrossRef]
57. Fay, N.P.; Bennett, R.A.; Hreinsdóttir, S. Contemporary vertical velocity of the central Basin and Range and uplift of the southern Sierra Nevada. *Geophys. Res. Lett.* **2008**, *35*, L20309. [CrossRef]
58. Mora-Páez, H.; Kellogg, J.N.; Freymueller, J.T.; Mencin, D.; Fernandes, R.M.S.; Diederix, H.; LaFemina, P.; Cardona-Piedrahita, L.; Lizarazo, S.; Peláez-Gaviria, J.-R.; et al. Crustal deformation in the northern Andes–A new GPS velocity field. *J. S. Am. Earth Sci.* **2019**, *89*, 76–91. [CrossRef]
59. Wang, G.; Liu, H.; Mattioli, G.S.; Braun, J.; Miller, M.M.; Feaux, K. Carib18: A stable geodetic reference frame for geological hazard monitoring in the caribbean region. *Remote Sens.* **2019**, *11*, 680. [CrossRef]
60. Jade, S.; Rao, H.J.R.; Vijayan, M.S.M.; Gaur, V.K.; Bhatt, B.C.; Kumar, K.; Jaganathan, S.; Ananda, M.B.; Kumar, P.D. GPS-derived deformation rates in northwestern Himalaya and Ladakh. *Int. J. Earth Sci.* **2011**, *100*, 1293–1301. [CrossRef]
61. Bisht, H.; Kotlia, B.S.; Kumar, K.; Dumka, R.K.; Taloor, A.K.; Upadhyay, R. GPS derived crustal velocity, tectonic deformation and strain in the Indian Himalayan arc. *Quat. Int.* **2021**, *575–576*, 141–152. [CrossRef]
62. Gülal, E.; Erdoğan, H.; Tiryakioğlu, I. Research on the stability analysis of GNSS reference stations network by time series analysis. *Digit. Signal Process. A Rev. J.* **2013**, *23*, 1945–1957. [CrossRef]
63. Bitharis, S.; Fotiou, A.; Pikridas, C.; Rossikopoulos, D. A new velocity field of greece based on seven years (2008–2014) continuously operating GPS station data. *Int. Assoc. Geod. Symp.* **2018**, *147*, 321–329.
64. Sánchez, L.; Völksen, C.; Sokolov, A.; Arenz, H.; Seitz, F. Present-day surface deformation of the Alpine region inferred from geodetic techniques. *Earth Syst. Sci. Data* **2018**, *10*, 1503–1526. [CrossRef]
65. Guo, W.; Wang, G.; Bao, Y.; Li, P.; Zhang, M.; Gong, Q.; Li, R.; Gao, Y.; Zhao, R.; Shen, S. Detection and monitoring of tunneling-induced riverbed deformation using gps and beidou: A case study. *Appl. Sci.* **2019**, *9*, 2759. [CrossRef]
66. Yu, J.; Yan, B.; Meng, X.; Shao, X.; Ye, H. Measurement of bridge dynamic responses using network-based real-time kinematic gnss technique. *J. Surv. Eng.* **2016**, *142*, 04015013. [CrossRef]
67. Jiang, W.; Liu, H.; Liu, W.; He, Y. CORS development for Xilongchi dam deformation monitoring. *Wuhan Daxue Xuebao (Xinxi Kexue Ban)/Geomat. Inf. Sci. Wuhan Univ.* **2012**, *37*, 949–952.
68. Jing-Xiang, G.; Hong, H. Advanced GNSS technology of mining deformation monitoring. *Procedia Earth Planet. Sci.* **2009**, *1*, 1081–1088. [CrossRef]
69. Guo, J.; Hu, J.; Li, B.; Zhou, L.; Wang, W. Land subsidence in Tianjin for 2015 to 2016 revealed by the analysis of Sentinel-1A with SBAS-InSAR. *J. Appl. Remote Sens.* **2017**, *11*, 026024. [CrossRef]
70. Zhang, T.; Shen, W.-B.; Wu, W.; Zhang, B.; Pan, Y. Recent surface deformation in the Tianjin area revealed by Sentinel-1A data. *Remote Sens.* **2019**, *11*, 130. [CrossRef]
71. Yalvac, S. Validating InSAR-SBAS results by means of different GNSS analysis techniques in medium- and high-grade deformation areas. *Environ. Monit. Assess.* **2020**, *192*, 120. [CrossRef]
72. Teunissen, P.J.G.; Odijk, D.; Zhang, B. PPP-RTK: Results of CORS network-based PPP with integer ambiguity resolution. *J. Aeronaut. Astronaut. Aviat.* **2010**, *42*, 223–230.

73. Zhang, B.; Teunissen, P.J.G.; Odijk, D. A novel un-differenced PPP-RTK concept. *J. Navig.* **2011**, *64* (Suppl. S1), S180–S191. [CrossRef]
74. Teunissen, P.J.G. The least-squares ambiguity decorrelation adjustment: A method for fast GPS integer ambiguity estimation. *J. Geod.* **1995**, *70*, 65–82. [CrossRef]
75. Eckl, M.C.; Snay, R.A.; Soler, T.; Cline, M.W.; Mader, G.L. Accuracy of GPS-derived relative positions as a function of interstation distance and observing-session duration. *J. Geod.* **2001**, *75*, 633–640. [CrossRef]
76. Feng, Y.; Rizos, C. Network-based geometry-free three carrier ambiguity resolution and phase bias calibration. *GPS Solut.* **2009**, *13*, 43–56. [CrossRef]
77. Eren, K.; Uzel, T.; Gulal, E.; Yildirim, O.; Cingoz, A. Results from a comprehensive global navigation satellite system test in the CORS-TR network: Case study. *J. Surv. Eng.* **2009**, *135*, 10–18. [CrossRef]
78. Li, B.; Shen, Y.; Feng, Y.; Gao, W.; Yang, L. GNSS ambiguity resolution with controllable failure rate for long baseline network RTK. *J. Geod.* **2014**, *88*, 99–112. [CrossRef]
79. Dabove, P.; Manzino, A.M.; Taglioretti, C. GNSS network products for post-processing positioning: Limitations and peculiarities. *Appl. Geomat.* **2014**, *6*, 27–36. [CrossRef]
80. Schwarz, C.R.; Snay, R.A.; Soler, T. Accuracy assessment of the national geodetic survey's OPUS-RS utility. *GPS Solut.* **2009**, *13*, 119–132. [CrossRef]
81. Aponte, J.; Meng, X.; Hill, C.; Moore, T.; Dodson, A.; Burbidge, M. Quality assessment of a network-based RTK GPS service in the UK Jose. *J. Appl. Geod.* **2009**, *3*, 25–34.
82. Edwards, S.J.; Clarke, P.J.; Penna, N.T.; Goebell, S. An examination of network RTK GPS services in Great Britain. *Surv. Rev.* **2010**, *42*, 107–121. [CrossRef]
83. Ding, W.; Tan, B.; Chen, Y.; Teferle, F.N.; Yuan, Y. Evaluation of a regional real-time precise positioning system based on GPS/BeiDou observations in Australia. *Adv. Space Res.* **2018**, *61*, 951–961. [CrossRef]
84. Jackson, J.; Davis, B.; Gebre-Egziabher, D. A performance assessment of low-cost RTK GNSS receivers. In Proceedings of the IEEE/ION Position, Location and Navigation Symposium—PLANS 2018, Monterey, CA, USA, 23–26 April 2018; pp. 642–649.
85. Netthonglang, C.; Thongtan, T.; Satirapod, C. GNSS Precise Positioning Determinations Using Smartphones. In Proceedings of the APCCAS 2019: IEEE Asia Pacific Conference on Circuits and Systems: Innovative CAS Towards Sustainable Energy and Technology Disruption, Bangkok, Thailand, 11–14 November 2019; pp. 401–404.
86. Pepe, M. Cors architecture and evaluation of positioning by low-cost gnss receiver. *Geod. Cartogr.* **2018**, *44*, 36–44. [CrossRef]
87. Forlani, G.; Dall'Asta, E.; Diotri, F.; di Cella, U.M.; Roncella, R.; Santise, M. Quality assessment of DSMs produced from UAV flights georeferenced with on-board RTK positioning. *Remote Sens.* **2018**, *10*, 311. [CrossRef]
88. Taddia, Y.; Stecchi, F.; Pellegrinelli, A. Coastal mapping using dji phantom 4 RTK in post-processing kinematic mode. *Drones* **2020**, *4*, 9. [CrossRef]
89. Zeybek, M. Accuracy assessment of direct georeferencing UAV images with onboard global navigation satellite system and comparison of CORS/RTK surveying methods. *Meas. Sci. Technol.* **2021**, *32*, 065402. [CrossRef]
90. Williams, S.D.P.; Bock, Y.; Fang, P.; Jamason, P.; Nikolaidis, R.M.; Prawirodirdjo, L.; Miller, M.; Johnson, D.J. Error analysis of continuous GPS position time series. *J. Geophys. Res. Solid Earth* **2004**, *109*, 1–19. [CrossRef]
91. Van Dierendonck, A.J.; Fenton, P.; Ford, T. Theory and Performance of Narrow Correlator Spacing in a GPS Receiver. *Navigation* **1992**, *39*, 265–283. [CrossRef]
92. Yang, B.; Yang, Z.; Tian, Z.; Liang, P. Weakening the Flicker Noise in GPS Vertical Coordinate Time Series Using Hybrid Approaches. *Remote Sens.* **2023**, *15*, 1716. [CrossRef]
93. Sun, C.; Cheong, J.W.; Dempster, A.G.; Zhao, H.; Feng, W. GNSS spoofing detection by means of signal quality monitoring (SQM) metric combinations. *IEEE Access* **2018**, *6*, 66428–66441. [CrossRef]
94. Andreotti, M.; Aquino, M.; Woolfson, M.; Walker, J.; Moore, T. Signal propagation analysis and signature extraction for GNSS indoor positioning. In Proceedings of the IEEE PLANS, Position Location and Navigation Symposium, Coronado, CA, USA, 25–27 April 2006; pp. 913–919.
95. Zhao, Q.; Zhang, K.; Yao, Y.; Li, X. A new troposphere tomography algorithm with a truncation factor model (TFM) for GNSS networks. *GPS Solut.* **2019**, *23*, 64. [CrossRef]
96. Tsugawa, T.; Saito, A.; Otsuka, Y.; Yamamoto, M. Damping of large-scale traveling ionospheric disturbances detected with GPS networks during the geomagnetic storm. *J. Geophys. Res. Space Phys.* **2003**, *108*, 1127. [CrossRef]
97. Komjathy, A.; Sparks, L.; Wilson, B.D.; Mannucci, A.J. Automated daily processing of more than 1000 ground-based GPS receivers for studying intense ionospheric storms. *Radio Sci.* **2005**, *40*, 1–11. [CrossRef]
98. Wielgosz, P.; Kashani, I.; Grejner-Brzezinska, D. Analysis of long-range network RTK during a severe ionospheric storm. *J. Geod.* **2005**, *79*, 524–531. [CrossRef]
99. Lee, J.; Pullen, S.; Datta-Barua, S.; Enge, P. Assessment of nominal ionosphere spatial decorrelation for LAAS. In Proceedings of the IEEE PLANS, Position Location and Navigation Symposium, Coronado, CA, USA, 25–27 April 2006; pp. 506–514.
100. Hong, C.-K.; Grejner-Brzezinska, D.A.; Kwon, J.H. Efficient GPS receiver DCB estimation for ionosphere modeling using satellite-receiver geometry changes. *Earth Planets Space* **2008**, *60*, e25–e28. [CrossRef]
101. Ji, S.; Chen, W.; Ding, X.; Zhao, C. Equatorial ionospheric zonal drift by monitoring local GPS reference networks. *J. Geophys. Res. Space Phys.* **2011**, *116*, A08310. [CrossRef]

102. Zhang, B.; Zhao, C.; Odolinski, R.; Liu, T. Functional model modification of precise point positioning considering the time-varying code biases of a receiver. *Satell. Navig.* **2021**, *2*, 11. [CrossRef]
103. Xiao, G.; Ou, J.; Liu, G.; Zhang, H. Construction of a regional precise tropospheric delay model based on improved BP neural network. *Acta Geophys. Sin.* **2018**, *61*, 3139–3148.
104. Graffigna, V.; Hernández-Pajares, M.; Gende, M.; Azpilicueta, F.; Antico, P. Interpretation of the Tropospheric Gradients Estimated with GPS During Hurricane Harvey. *Earth Space Sci.* **2019**, *6*, 1348–1365. [CrossRef]
105. Devoti, R.; D'Agostino, N.; Serpelloni, E.; Pietrantonio, G.; Riguzzi, F.; Avallone, A.; Cavaliere, A.; Cheloni, D.; Cecere, G.; D'Ambrosio, C.; et al. A combined velocity field of the mediterranean region. *Ann. Geophys.* **2017**, *60*, S0215. [CrossRef]
106. Avallone, A.; Selvaggi, G.; D'Anastasio, E.; D'Agostino, N.; Pietrantonio, G.; Riguzzi, F.; Serpelloni, E.; Anzidei, M.; Casula, G.; Cecere, G.; et al. The RING network: Improvements to a GPS velocity field in the central Mediterranean. *Ann. Geophys.* **2010**, *53*, 39–54. [CrossRef]
107. Siornet GPS Network ISPRA. Available online: https://www.isprambiente.gov.it/en/projects/soil-and-territory/siornet-permanent-gps-network/siornet-permanent-gps-network (accessed on 22 September 2023).
108. Dardanelli, G.; Lo Brutto, M.; Pipitone, C. GNSS Cors Network of the University of Palermo: Design and First Analysis of Data. *Geogr. Tech.* **2020**, *15*, 43–69. [CrossRef]
109. Topcon GNSS Network. Available online: https://www.topconpositioning.com/surveying/gnss-reference-network (accessed on 22 September 2023).
110. Dardanelli, G.; Sansone Santamaria, A. RFI: A case study of the University of Palermo. In Proceedings of the 5th International Conference and Exhibition Melaha (Egypt), Cairo, Egypt, 3–5 May 2010.
111. Dardanelli, G.; La Loggia, G.; Perfetti, N.; Capodici, F.; Puccio, L.; Maltese, A. Monitoring displacements of an earthen dam using GNSS and remote sensing. In *Proceedings of SPIE—The International Society for Optical Engineering*; SPIE: Bellingham, WA, USA, 2014.
112. Dardanelli, G.; Pipitone, C. Hydraulic models and finite elements for monitoring of an earth dam, by using GNSS techniques. *Period. Polytech. Civ. Eng.* **2017**, *61*, 421–433. [CrossRef]
113. Pipitone, C.; Maltese, A.; Dardanelli, G.; Lo Brutto, M.; La Loggia, G. Monitoring water surface and level of a reservoir using different remote sensing approaches and comparison with dam displacements evaluated via GNSS. *Remote Sens.* **2018**, *10*, 71. [CrossRef]
114. Maltese, A.; Pipitone, C.; Dardanelli, G.; Capodici, F.; Muller, J.-P. Toward a Comprehensive Dam Monitoring: On-Site and Remote-Retrieved Forcing Factors and Resulting Displacements (GNSS and PS–InSAR). *Remote Sens.* **2021**, *13*, 1543. [CrossRef]
115. Stocchi, P.; Antonioli, F.; Montagna, P.; Pepe, F.; Lo Presti, V.; Caruso, A.; Corradino, M.; Dardanelli, G.; Renda, P.; Frank, N.; et al. A stalactite record of four relative sea-level highstands during the Middle Pleistocene Transition. *Quat. Sci. Rev.* **2017**, *173*, 92–100. [CrossRef]
116. Parrino, N.; Pepe, F.; Burrato, P.; Dardanelli, G.; Corradino, M.; Pipitone, C.; Morticelli, M.G.; Sulli, A.; Di Maggio, C. Elusive active faults in a low strain rate region (Sicily, Italy): Hints from a multidisciplinary land-to-sea approach. *Tectonophysics* **2022**, *839*, 229520. [CrossRef]
117. Pipitone, C.; Dardanelli, G.; Lo Brutto, M.; Bruno, V.; Mattia, M.; Guglielmino, F.; Rossi, M.; Barreca, G. Use of CORS Time Series for Geodynamics Applications in Western Sicily (Italy). *Commun. Comput. Inf. Sci.* **2020**, *1246*, 61–76.
118. Barreca, G.; Bruno, V.; Dardanelli, G.; Guglielmino, F.; Lo Brutto, M.; Mattia, M.; Pipitone, C.; Rossi, M. An integrated geodetic and InSAR technique for the monitoring and detection of active faulting in southwestern Sicily. *Ann. Geophys.* **2020**, *63*, EP03. [CrossRef]
119. Dardanelli, G.; Paliaga, S.; Allegra, M.; Carella, M.; Giammarresi, V. Geomatic applications tourban park in palermo. *Geogr. Tech.* **2015**, *10*, 28–43.
120. Dardanelli, G.; Carella, M. Integrated surveyng with mobile mapping system, egnos, ntrk and laser technologies in the park "Ninni Cassara" in Palermo. *ISPRS Ann. Photogramm. Remote Sens. Spat. Inf. Sci.* **2013**, *2*, 95–100. [CrossRef]
121. Sferlazza, S.; Maltese, A.; Dardanelli, G.; La Mela Veca, D.S. Optimizing the Sampling Area across an Old-Growth Forest via UAV-Borne Laser Scanning, GNSS, and Radial Surveying. *ISPRS Int. J. Geo-Inf.* **2022**, *11*, 168. [CrossRef]
122. Angrisano, A.; Dardanelli, G.; Innac, A.; Pisciotta, A.; Pipitone, C.; Gaglione, S. Performance assessment of PPP surveys with open source software using the GNSS GPS-GLONASS-Galileo constellations. *Appl. Sci.* **2020**, *10*, 5420. [CrossRef]
123. Dardanelli, G.; Pipitone, C. The effects of cors network geometry and differential nrtk corrections on gnss solutions. *Geogr. Tech.* **2021**, *16*, 56–69. [CrossRef]
124. Catania, P.; Comparetti, A.; Febo, P.; Morello, G.; Orlando, S.; Roma, E.; Vallone, M. Positioning accuracy comparison of GNSS receivers used for mapping and guidance of agricultural machines. *Agronomy* **2020**, *10*, 924. [CrossRef]
125. Dardanelli, G.; Maltese, A.; Pipitone, C.; Pisciotta, A.; Lo Brutto, M. Nrtk, ppp or static, that is the question. Testing different positioning solutions for gnss survey. *Remote Sens.* **2021**, *13*, 1406. [CrossRef]
126. Dardanelli, G.; Maltese, A. On the Accuracy of Cadastral Marks: Statistical Analyses to Assess the Congruence among GNSS-Based Positioning and Official Maps. *Remote Sens.* **2022**, *14*, 4086. [CrossRef]
127. Ammoscato, A.; Corsale, R.; Dardanelli, G.; Scianna, A.; Villa, B. GPS-GIS integrated system for electromagnetic pollution. *Int. Arch. Photogramm. Remote Sens. Spat. Inf. Sci. ISPRS Arch.* **2008**, *37*, 491–497.

128. Dardanelli, G.; Marretta, R.; Santamaria, A.S.; Streva, A.; Lo Brutto, M.; Maltese, A. Analysis of technical criticalities for GIS modelling an Urban noise. *Geogr. Tech.* **2017**, *12*, 41–61. [CrossRef]
129. White, A.M.; Gardner, W.P.; Borsa, A.A.; Argus, D.F.; Martens, H.R. A Review of GNSS/GPS in Hydrogeodesy: Hydrologic Loading Applications and Their Implications for Water Resource Research. *Water Resour. Res.* **2022**, *58*, e2022WR032078. [CrossRef]